 doi:10.20944/preprints202206.0382.v1

Article

Fibres as Replacement of Horizontal Ties in Compressed Reinforced Concrete Elements: Experimental Study

Ulvis Skadins [1] 0000-0002-4430-735X

[1] Lead researcher; ulvis.skadins@llu.lv

Abstract: Steel fibres provides ductility to concrete structures. This in turn gives possibility to replace or reduce conventional reinforcement in structural elements. In this study the focus is on structural walls and the fibres as potential replacement for horizontal reinforcement in areas where vertical re-bars are needed. An experimental study was conducted, in which prismatic specimens with longitudinal re-bars were subjected to centric loading. Ten samples with 12 specimens in each were tested. The parameters considered were: fibre content, concrete cover for the longitudinal bars, and presence of stirrups. Self-compacting concrete with 30 and 60 kg/m^3 steel fibres was used. The influence of fibres on maximum load, stiffness, and ductility of the specimens is evaluated. The results show that fibres eliminated brittle collapse and spalling of concrete at failure. Samples with fibres tend to have reduced maximum force and stiffness but increased ductility. The specimens with fibre content of 60 kg/m^3 showed more ductile behaviour than the ones with minimum amount of conventional stirrups. The study suggests that combination of steel fibres and conventional re-bars can lead to less qualitative compactness of the self-compacting concrete, which in turn may reduce load bearing capacity and stiffness of the structure.

Keywords: steel fibres; stirrups; concrete walls; self-compacting concrete; buckling of re-bars

1. Introduction

The present study is a part of a research project [1], in which the effect of steel fibres in concrete wall structures is being investigated. The main objective of the project is to understand if it is possible to replace conventional reinforcement with short steel fibres in structural walls. As a result, reduced production costs of concrete walls due to simplified reinforcement arrangements could be achieved, even if the replacement can be done in part.

Simple concrete walls have comparatively high load bearing capacity and in many cases (e.g. low rise buildings or walls of upper floors) reinforcement bars are provided to prevent shrinkage cracking or add some ductility, but do not have any load bearing function. However, walls can have complex geometry due to door or window openings. That can lead to heavily loaded areas, where longitudinal bars should be provided to ensure the necessary bearing capacity. In such areas horizontal tie bars are needed to prevent longitudinal bars from buckling. The ties, if properly placed, increases the effectiveness of concrete core between the longitudinal bars, acting as lateral confinement. If the tie bars are replaced by fibres, the arrangement of the conventional reinforcement would be simplified considerably.

Effect of fibres in compressed structural concrete elements is noticed by several researchers. Zhang et al [2] have found that fibres improve the behaviour of hollow concrete bridge piers and suggest that transverse reinforcement can be partly substituted by fibres of seismic design. Fantilli et al [3] have found that adding 0.9% steel fibres to concrete columns gives similar effect of 1.0 MPa lateral (confining) pressure. Ganesan and Ramana Murthy [4] have suggested that some amount of confining reinforcement can be replaced by certain amount of fibres. Their study showed that concrete columns with 0.6% confining stirrups and 1.5% steel fibres have the same effect as plain concrete

Preprints (www.preprints.org) | NOT PEER-REVIEWED | Posted: 28 June 2022 doi:10.20944/preprints202206.0382.v1

with 1.6% stirrups. Pereiro-Barceló and Bonet [5] measured strains on re-bars subjected to buckling and found that strains, at which the reinforcement buckles, increases with the increase of fibre content. There is a recent study [6] in which concrete columns confined by a layer of special fibre reinforced composite called Engineered Cementitious Composite (ECC) are investigated and a positive effect on the axial load bearing capacity was found.

Although there are several valuable experimental studies performed, and the effect of fibres in compressed structural elements described, it hasn't resulted in practical design rules. Design guidelines prepared by SFRC Consortium [7] states that "the effect of steel fibres may not be considered with respect to transverse reinforcement of columns." No additional rules for walls are given in this standard. The Swedish standard SS 812310:2014 [8] do not provide for any design or detailing rules specific to SFRC walls or columns.

The aim of this study is to contribute to the current knowledge about the influence of steel fibres on the behaviour of concrete walls and columns under compressive loading and to compare the effect of fibres with the minimum required horizontal ties. There are several distinctive approaches used in this study if compared to other authors. First, large amount of specimens (120 prisms) are tested to increase the statistical power of the results. Second, the specimens are manufactured in a concrete plant not in lab, to capture issues related to real life production process. Third, the effect of fibres for specimens with no stirrups are investigated here, while combined effect of fibres and stirrups are studied in the papers mentioned above.

2. Materials and Methods

2.1. Types of specimens

Prism-type specimens with four longitudinal re-bars and steel end-plates were produced. The main parameters to be analysed are the amount of fibres and concrete cover of the longitudinal reinforcement bars. Two additional samples with conventional stirrups were manufactured. All together 10 different samples with 12 specimens in each were produced. The samples are labelled with a capital letter "P" followed by numbers #-#, the first of which refers to material, while the other – to the arrangement of the conventional reinforcement, denoted as group. A summary of the samples is given in Table 1. Dimensions and arrangement of conventional reinforcement used in the specimens is shown in Figure 1.

Table 1. Test samples.

Sample name	Material	Reinf. group	Test date	Fibre content kg/m^3	Distance to re-bars, mm	Stirrups
P1-1	PC	1	01.21.2021	0	30	-
P1-2	PC	2	01.20.2021	0	40	-
P1-3	PC	3	01.22.2021	0	50	-
P1-4	PC	4	01.22.2021	0	30	+
P1-5	PC	5	01.21.2021	0	50	+
P2-1	F30	1	01.19.2021	30	30	-
P2-3	F30	3	01.19.2021	30	50	-
P3-1	F60	1	01.14.2021	60	30	-
P3-2	F60	2	01.14.2021	60	40	-
P3-3	F60	3	01.15.2021	60	50	-

All the specimens are grouped in 5 groups, depending on the arrangement of the conventional reinforcement. In groups 1, 2, and 3 there are specimens with longitudinal re-bars only (see Figure 1 (a)), having different distances of the bars from the side of the specimens c: 30 mm, 40 mm, and 50 mm, respectively. In groups 4 and 5 stirrups

Preprints (www.preprints.org) | NOT PEER-REVIEWED | Posted: 28 June 2022 doi:10.20944/preprints202206.0382.v1

are included according to Figure 1 (b) and (d). Values of the distance *c* are 30 mm and 50 mm, respectively.

Two steel plates are welded to the longitudinal re-bars at both ends of the specimen. This is done to ensure that the applied load is transferred to all four steel bars directly. It is also expected that in such a way the variation in test results caused by misplacement of reinforcement and unevenness of loading surfaces is minimised. In all of the samples ribbed bars of diameter 12 mm are used as the longitudinal reinforcement. The correct position of the bars are ensured by the end plates with pre-drilled holes. The bars were fixed in the holes and welded to the plates. The outside of the plates were smooth to reduce undesirable effect of local imperfections. Nominal dimensions of the specimens were 150×150×480 mm including the thickness of both end-plates 2×15 mm. Actual dimensions of each specimen were measured and used in the evaluation of the results. The measurements are available in an open-access database [1].

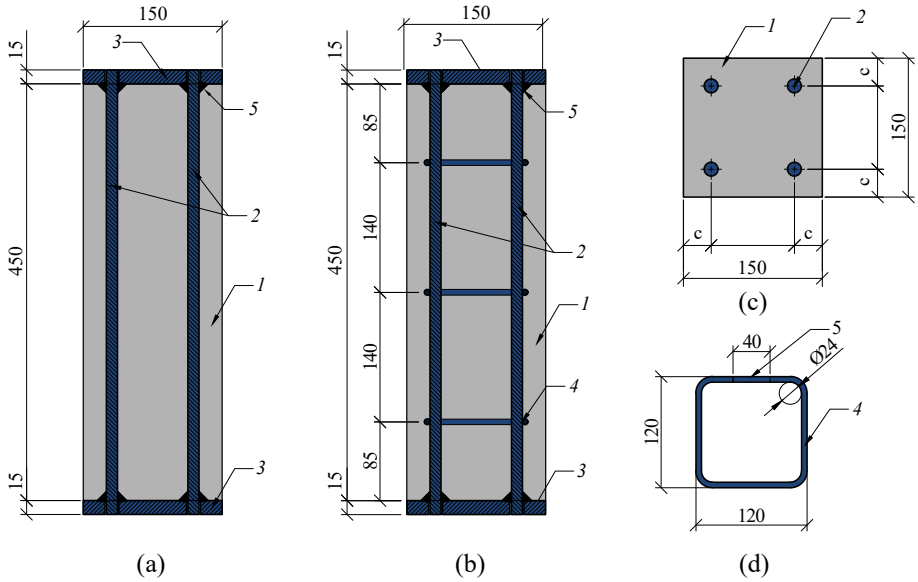

Figure 1. Specimens: (**a**) group 1 to 3; (**b**) group 4 and 5; (**c**) cross section; (**d**) geometry of stirrups; *1* – concrete; *2* – longitudinal reinforcement ⌀12 mm; *3* – steel end-plates; *4* – stirrups ⌀6 mm; *5* – welded joint; c – distance 30 mm, 40 mm, and 50 mm.

2.2. Materials

Self-compacting concrete was used. All the specimens were made in pre-cast concrete plant "Dzelzsbetons MB" in Liepaja, Latvia. Casting method was the same as for normal concrete – the concrete was falling in horizontal moulds on a casting table from vertical distance of around 0.5 m as shown in Figure 2(b). No vibration was applied. Detailed description of the materials used in this study is available in the project's database [1].

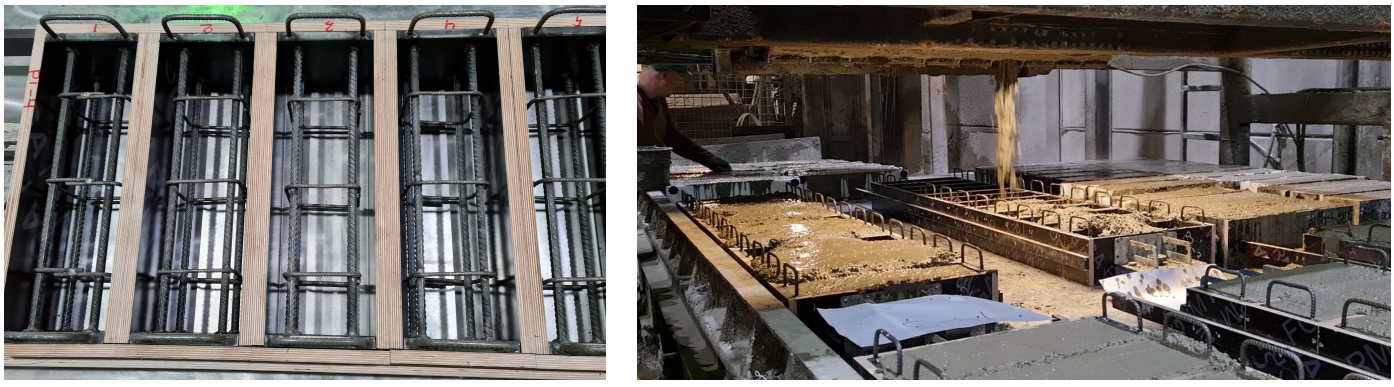

(a) (b)

Figure 2. Manufacturing of the specimens in pre-cast concrete plant: (**a**) prepared moulds; (**b**) casting process.

Preprints (www.preprints.org) | NOT PEER-REVIEWED | Posted: 28 June 2022 doi:10.20944/preprints202206.0382.v1

Three types of materials were used in this study: 1) plain concrete (PC); 2) steel fibre reinforced concrete (SFRC) with fibre content 30 kg/m^3 (F30); 3) SFRC with fibre content 60 kg/m^3 (F60). The following properties of concrete and SFRC are determined by laboratory tests: 1) compressive strength of standard cube specimens according to EN 12390-3 [9]; 2) flexural tensile strength for plain concrete according to EN 12390-5 [10]; 3) flexural tensile strength at the limit of proportionality (LOP) and residual flexural strength of SFRC according to EN 14651 [11]. Concrete tensile strength is derived from the flexural tensile strength based on the formula given in Model Code 2010 [12].

$$f_{ctm} = f_{ctm,fl}\,\alpha_{fl} = \frac{0.06 f_{ctm,fl}\, h^{0.7}}{1 + 0.06\, h^{0.7}}\,, \tag{1}$$

where $f_{ctm,fl}$ is flexural tensile strength or strength at LOP (f_{RL}) of the tested prisms; h is the total depth of the member or the distance from the tip of the notch to the top of the specimen (h_{sp}) for SFRC. Modulus of elasticity for concrete is calculated based on the compressive strength according to Eurocode 2 (EC2) [13]. The material properties are given in Table 2 and Table 3. The scatter of the concrete compressive and tensile strength test data is represented in form of box-plots in Figure 3. The *load–CMOD* (Crack Mouth Opening Distance) curves of SFRC standard prisms are plotted in Figure 4.

Table 2. Material properties.

Material	Label	Fibre content, kg/m^3	Fibre content, %	$f_{cube.m}$, MPa	CoV	E_{cm}, GPa	f_{ctm}, MPa	CoV
1	PC	0	0	41.25	0.03	33.655	3.85	0.07
2	F30	30	≈ 0.4	44.56	0.03	34.442	2.86	0.05
3	F60	60	≈ 0.8	43.09	0.03	34.097	2.68	0.07

CoV – Coefficient of variance

Table 3. Material properties of SFRC.

Mat. label	LOP / residual strength, MPa					Coefficients of variance				
	$f_{RL.m}$	$f_{R1.m}$	$f_{R2.m}$	$f_{R3.m}$	$f_{R4.m}$	CoV_L	CoV_1	CoV_2	CoV_3	CoV_4
F30	4.49	3.38	3.76	3.80	3.79	0.05	0.24	0.24	0.24	0.22
F60	4.24	4.84	5.21	4.71	4.15	0.07	0.27	0.24	0.21	0.18

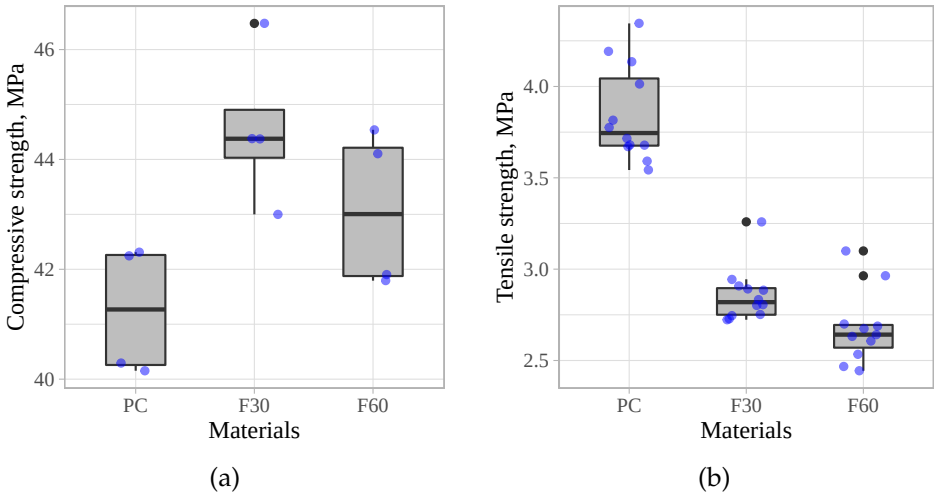

Figure 3. Material properties: (**a**) compressive strength; (**b**) flexural tensile strength.

Preprints (www.preprints.org) | NOT PEER-REVIEWED | Posted: 28 June 2022 doi:10.20944/preprints202206.0382.v1

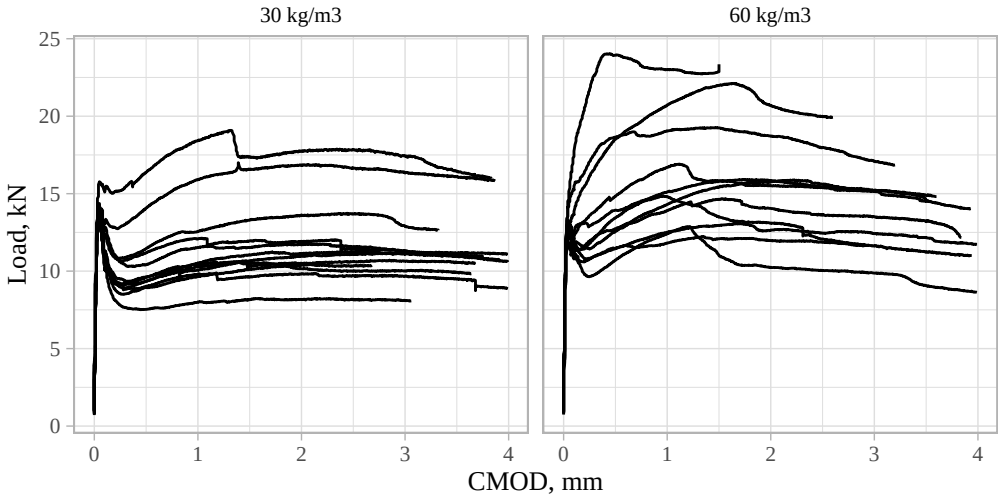

Figure 4. Force–CMOD curves of SFRC standard prisms.

2.3. Test set-up and loading

All of the specimens were loaded in centric compression in a hydraulic testing machine ALPHA 10-3000 (Form+Test) with closed-loop control system. The loading speed was set 10 kN/s till load level of 800 kN, after which speed of piston displacement was controlled 0.025 mm/s till failure of the specimen. For specimens in samples P3-1 and P3-2 the loading was controlled by force with speed 10 kN/s till the failure. This resulted in loss of the test data after maximum force was reached. Therefore the post-peak behaviour of these specimens are not included in further analysis.

Vertical and horizontal strains were measured for two specimens (P1-2-10 and P2-3-11) for control purposes. Strain guages HBM 1-LY41-20/120 with grid length 20 mm were used at the middle of each vertical side of the specimens. The test set-up is shown in Figure 5.

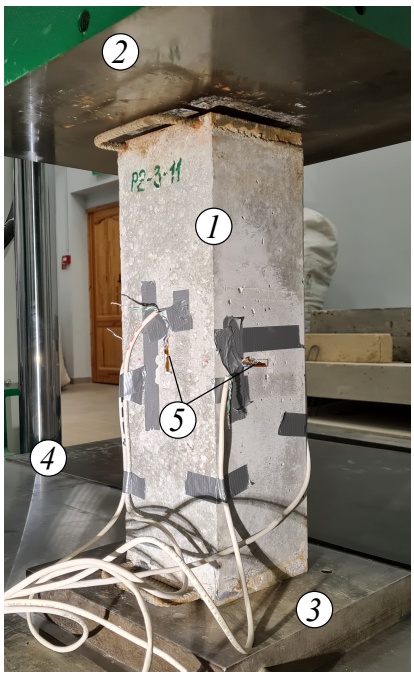

Figure 5. Test set-up: 1 – test specimen; 2 – loading head with ball-seat; 3 – base plate; 4 – machine frame; 5 – strain gauges (for two specimens only).

Preprints (www.preprints.org) | NOT PEER-REVIEWED | Posted: 28 June 2022 doi:10.20944/preprints202206.0382.v1

2.4. Methods of evaluation

The effect of fibres is evaluated by comparing the main mechanical properties of the specimens obtained from the testing: maximum load, axial stiffness, ductility. To compare the results of samples with different material and geometrical properties, relative and normalised values are used.

2.4.1. Maximum load

The maximum load was compared by introducing *relative force* that is calculated considering actual geometrical properties of each specimen and material properties of the sample. Presence of the longitudinal reinforcement was also taken into account. The relative force for each specimen is calculated by the following equation:

$$F_{rel,i} = \frac{F_{max,i}}{f_{cube.m,i} A_{cm,i} + f_y A_s}, \tag{2}$$

where $F_{max,i}$ is maximum load bearing capacity of the specimen; $f_{cube.m,i}$ is the mean value of concrete cube compressive strength; $A_{cm,i}$ cross-section of the specimen measured at the middle of specimens; f_y yield strength of the conventional reinforcement taken as 500 MPa; A_s is total cross-sectional area of vertical reinforcement bars. In all cases $A_s = 452.4$ mm^2, corresponding to 4⌀12 mm, is assumed.

2.4.2. Axial stiffness

The overall stiffness of a specimen was obtained using the procedure given in Figure 6. First the original *force–piston displacement* curves were converted by removing the effect of frame deformations. The stiffness of the machine frame was evaluated by recording *force–piston displacement* data while loading the frame without any specimen. To adjust the vertical deformations of the tested specimens, the following equation was derived:

$$u_i = u_{i,init} - F_i \frac{A + B}{F_i + C}, \tag{3}$$

where u_i is vertical displacement of the specimen; $u_{i,init}$ is the vertical displacement recorded during the test that includes the deformations of the frame; F_i is load recorded at the corresponding displacement; A, B, and C are coefficients describing the stiffness of the machine frame: 0.000974, 0.2, and 260.0, respectively.

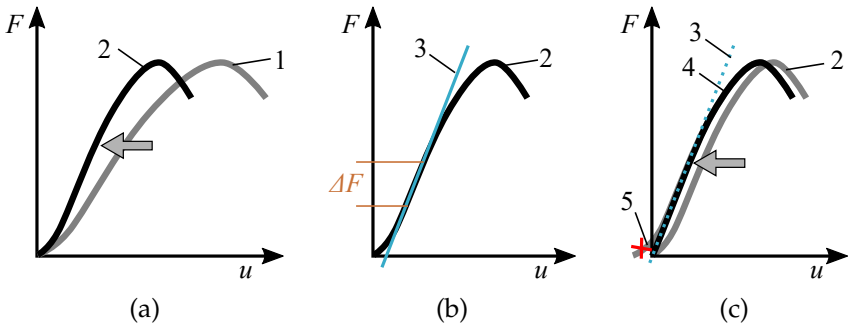

Figure 6. Stiffness evaluation procedure: 1 – original *force–piston displacement* curve; 2 – curve with frame deformations removed; 3 – stiffness secant giving maximum angle with horizontal axis; 4 – converted *force–displacement* curve used in further analysis; 5 – initial imperfections removed; ΔF – force difference between points of the stiffness secant.

The stiffness of each specimen is evaluated as secant going through two points on the *force–displacement* curve with a distance ΔF equal to 200 kN. The lowest point was obtained by iteration, for which the stiffness secant has the largest angle with the horizontal axis (Figure 6 (b)). The iteration was done by steps equal to 50 kN, starting

Preprints (www.preprints.org) | NOT PEER-REVIEWED | Posted: 28 June 2022 doi:10.20944/preprints202206.0382.v1

from zero and finishing at a level at which the upper point reaches 90% of the peak load. Other ΔF values (150, 250, 300, 350, 400) were also analysed. In all cases the tendencies of the results were the same, while the 150 kN range was more sensitive to the parameters in the procedure applied.

After defining the secant, the curves of each specimen were moved so that the secant would intersect horizontal and vertical axis at zero point. All the data points before/above the secant were considered invalid, representing initial imperfections, and therefore removed (Figure 6 (c)).

To compare the stiffness between different samples and specimens, a relative stiffness value D_{rel} was introduced. It was obtained by dividing the experimentally determined stiffness D_{exp} by a theoretical stiffness D_{theor}:

$$D_{rel,i} = \frac{D_{exp,i}}{D_{theor,i}} = \frac{\Delta F\, h_i}{\Delta u_i\, (E_{cm,i} A_{cm,i} + E_s A_s)}, \tag{4}$$

where Δu_i – difference of displacements between the points of the stiffness secant; h_i – height of the specimen considered; $E_{cm,i}$ – concrete secant modulus of elasticity for the sample considered (see Table 2); E_s – modulus of elasticity for reinforcement steel taken equal to 200 GPa.

2.4.3. Ductility

Ductility of the specimens was compared by means of the area under the converted *load-displacement* curve. The comparison was done for all but samples S3-1 and S3-2. As mentioned before, the loading of the specimens in these samples was controlled only by force. Therefore the post-peak behaviour is abrupt and cannot be compared to other samples, for which the post-peak loading was controlled by displacement.

To compare the ductility between specimens, the *force–displacement* curves were normalised by dividing each recorded load value by the maximum load of the specimen F_i/F_{max} and each displacement value by the displacement at the maximum load u_i/u_{max} (see Figure 7 (a)).

The end of the *force–displacement* curve is assumed at the moment, when a rapid drop of the force begins. The measurements obtained in this phase are no reliable and therefore excluded (see Figure 7 (b)). If residual load bearing capacity of a specimen, after the first drop of the force, was captured, then the range was extended till the second drop of the force (Figure 7 (c)).

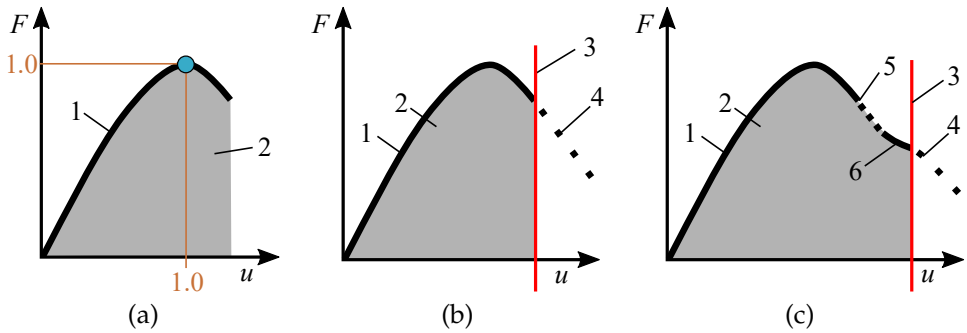

Figure 7. Ductility evaluation: 1 – converted *force–displacement* curve; 2 – area under the curve; 3 – boundary line for the area representing ductility; 4 – unreliable data points excluded from the evaluation; 5 – first drop of the force; 6 – residual capacity.

3. Results

Force–displacement behaviour was obtained for each specimen. Relative forces calculated by Equation (2) versus vertical displacement are plotted in Figure 8 for each sample. In the figure, data range (gray), mean curve (black), and outliers (gray dots)

Preprints (www.preprints.org) | NOT PEER-REVIEWED | Posted: 28 June 2022 doi:10.20944/preprints202206.0382.v1

are shown. The mean *force–displacement* curves are compared for samples with different concrete cover in Figure 10.

The outliers were defined by means of two properties: stiffness and maximum force, giving the values lower/greater than the first quartile minus/plus 1.5 times the inter quartile range. These specimens are excluded from further analysis. In case of stiffness, the specimens tagged as outliers varied depending on the value of ΔF (see Figure 6 (b)). Therefore only those specimens were considered outliers that fell into this category for all the ΔF values considered.

Data range and mean values of the normalised *force–displacement* curves obtained by the procedure given in Section 2.4.3, are represented in Figure 9. The mean values of the normalised *force–displacement* curves are compared in Figure 11.

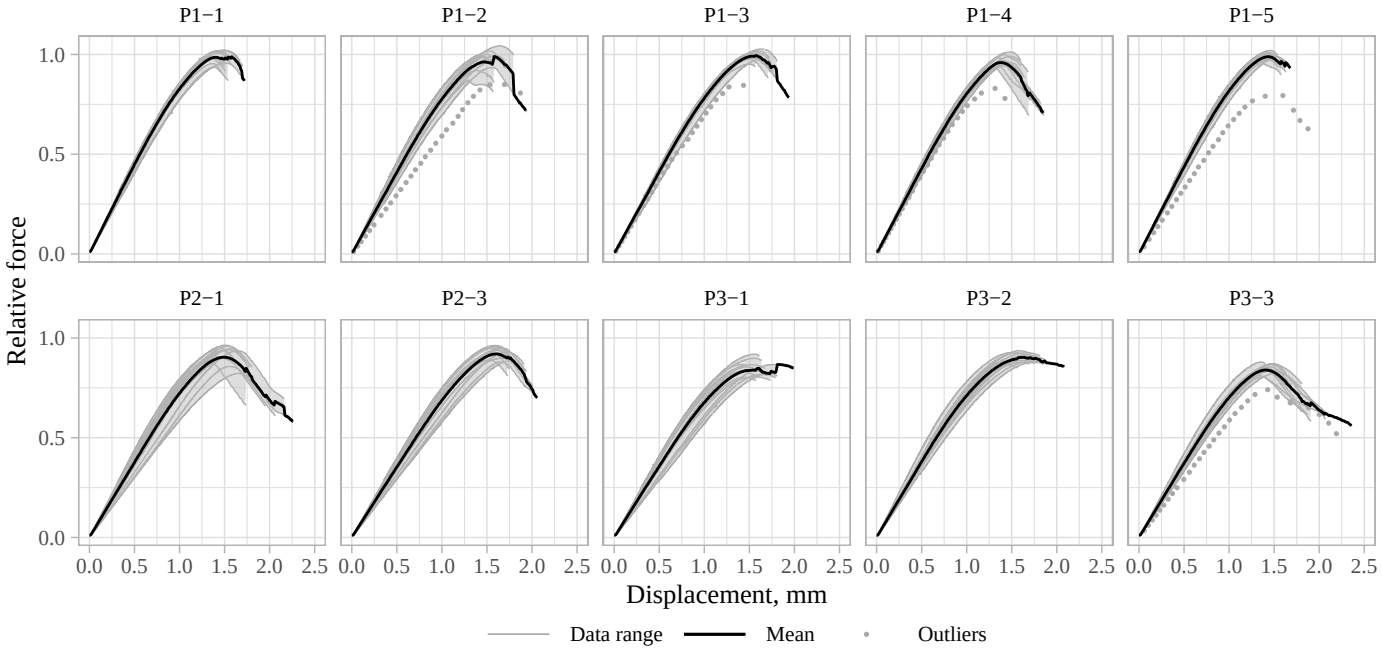

Figure 8. Relative force versus vertical displacement.

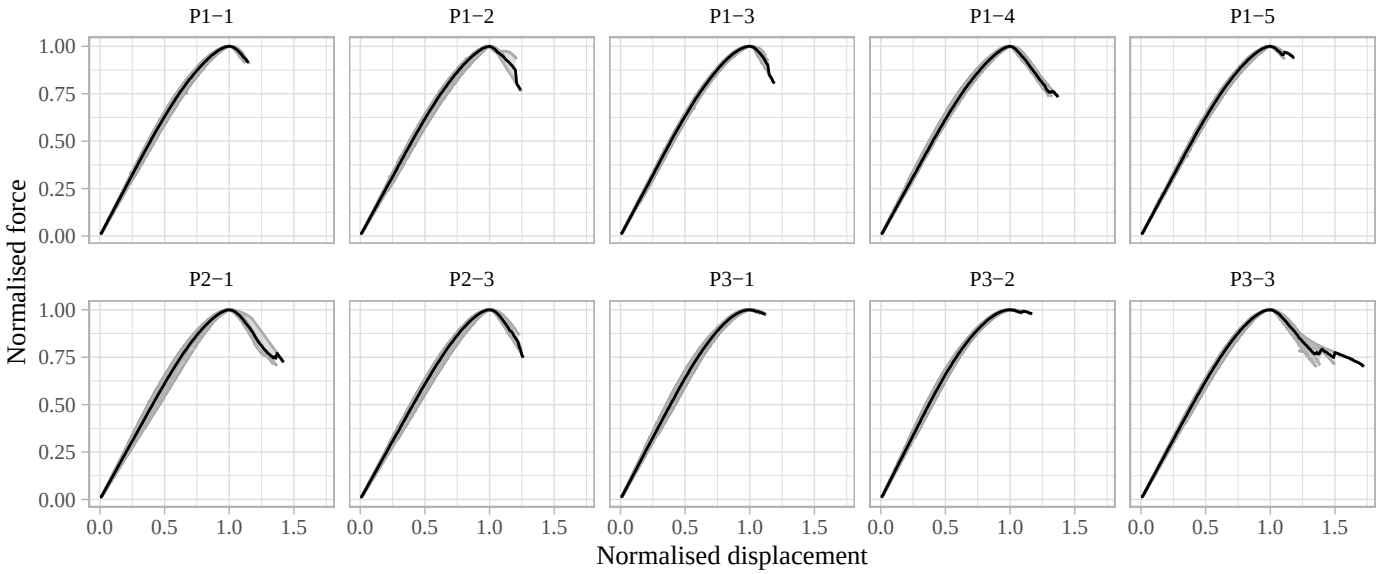

Figure 9. Normalised *force–displacement* diagrams.

Preprints (www.preprints.org) | NOT PEER-REVIEWED | Posted: 28 June 2022 doi:10.20944/preprints202206.0382.v1

The first tendencies that can be seen from the *force–displacement* diagrams, show that specimens with steel fibres 30 kg/m^3 and 60 kg/m^3 ($\approx$ 0.4% – 0.8%) tend to have smaller both stiffness and the maximum force, but there is an increase in ductility. The samples with minimum required amount of stirrups have the same behaviour as the samples with plain concrete, if axial stiffness or maximum force is compared. Stirrups as well as fibres improves ductility of the specimens under compression. However, the effect of stirrups depends on the concrete cover or the ratio of the volume enclosed by the stirrups to the concrete volume surrounding them. There is no increased ductility for specimens with 50 mm concrete cover. On the other hand, the effect of fibres is similar for both 30 mm and 50 mm covers. The effect of fibres on these properties are discussed in more detail in section 4.2. Two specimens representing typical failure modes of each sample are given in Figure 13.

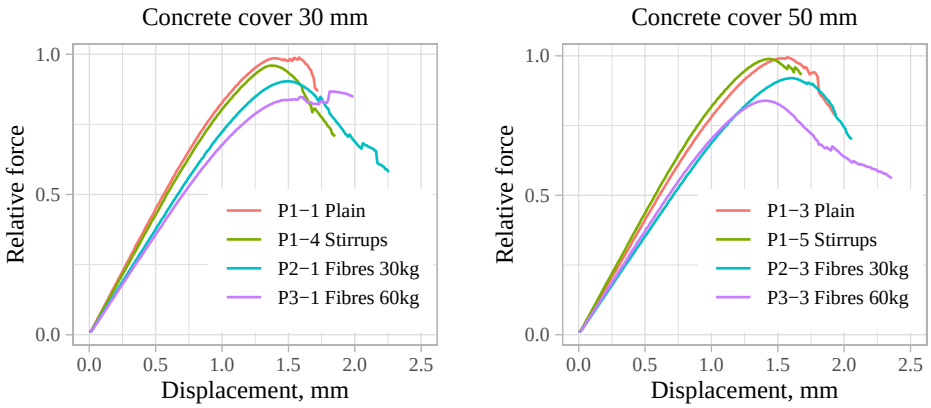

Figure 10. Mean values of relative force versus vertical displacement for samples with concrete covers: 30 mm and 50 mm.

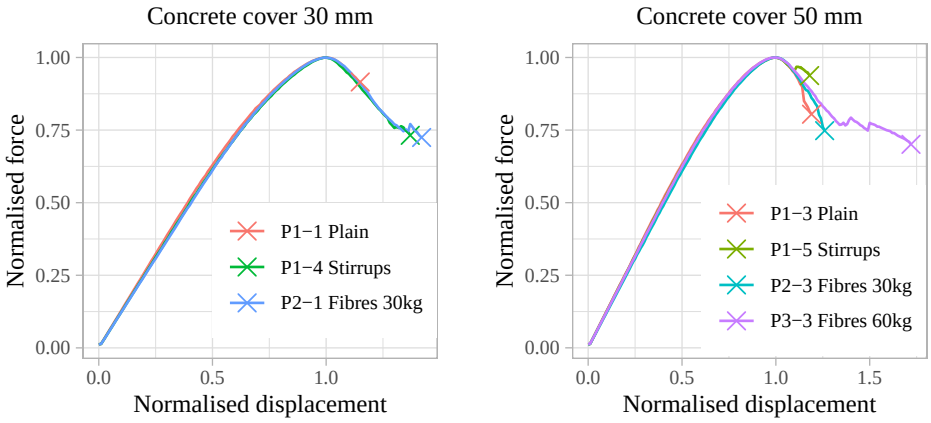

Figure 11. Mean values of normalised *force–displacement* diagrams for samples with concrete covers: 30 mm and 50 mm.

Two specimens (P1-2-10 and P2-3-11) were used to evaluate the *overall stiffness* used in this analysis. *Force versus strain* diagrams obtained by two methods are plotted in Figure 12. The blue data points represent "total strains" calculated as the overall vertical displacement obtained by the method described in Section 2.4.2 and divided by the overall height of the specimens. The black data points show the strains measured by strain gauges at the middle of the specimen. The *total strains* are $\approx$1.5 times larger than the ones measured at the middle of the specimens.

Preprints (www.preprints.org) | NOT PEER-REVIEWED | Posted: 28 June 2022 doi:10.20944/preprints202206.0382.v1

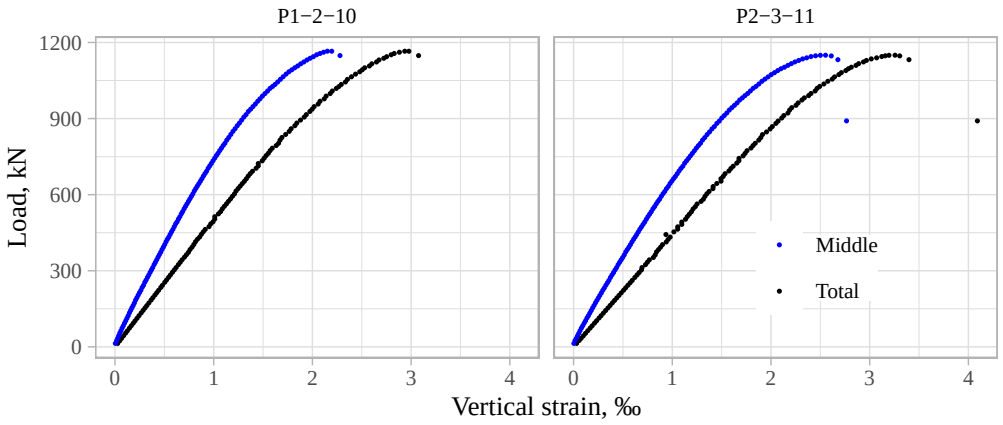

Figure 12. Force versus vertical strain measured by strain gauges at the middle of specimens and total strains in case of specimens P1-2-10 and P2-3-11.

P1-1-1 **P1-1**-8 **P1-2**-1 **P1-2**-5

P1-3-3 **P1-3**-5 **P1-4**-7 **P1-4**-8

Figure 13. Typical failure modes of the tested samples: two specimens from each sample.

Preprints (www.preprints.org) | NOT PEER-REVIEWED | Posted: 28 June 2022 doi:10.20944/preprints202206.0382.v1

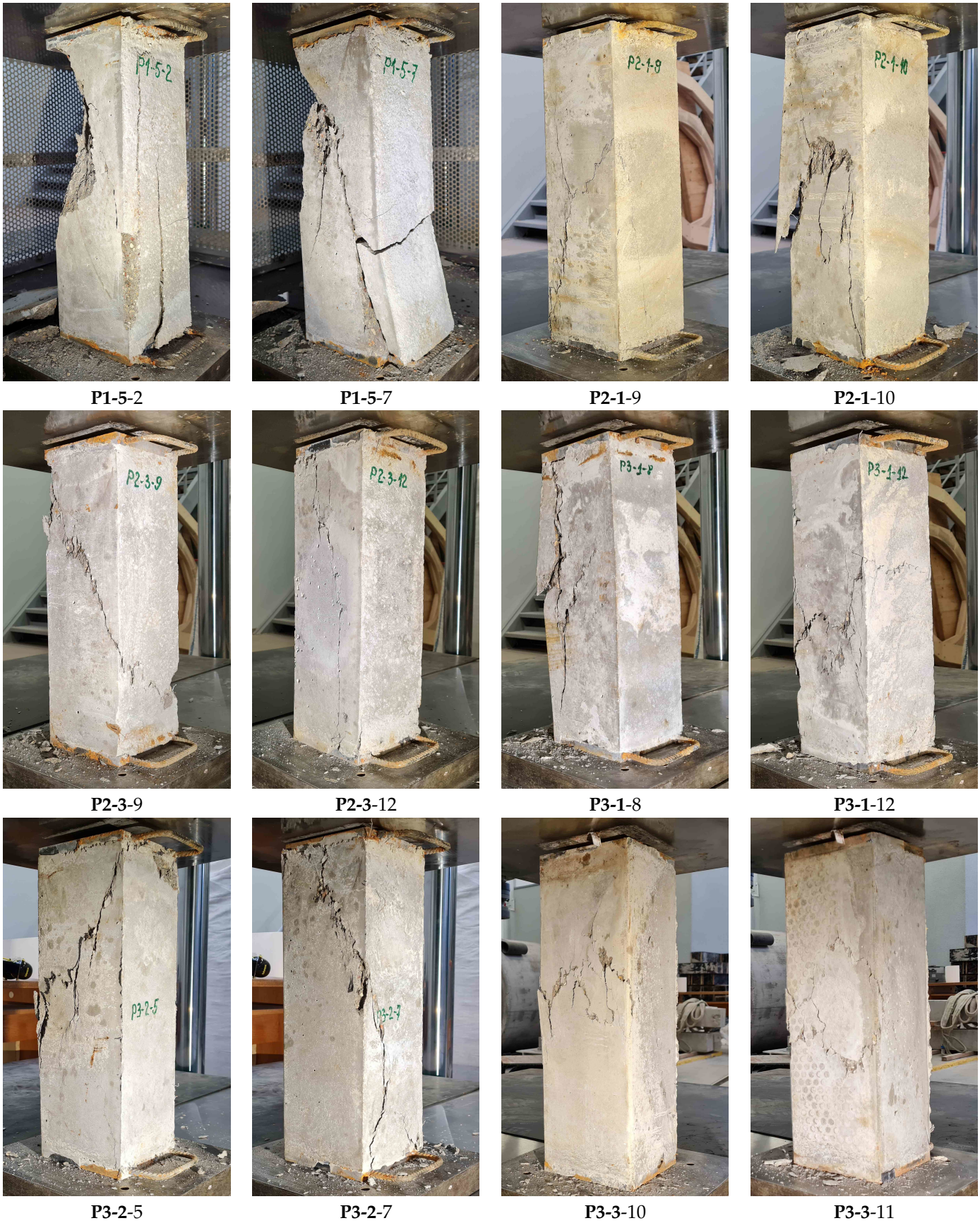

P1-5-2 **P1-5**-7 **P2-1**-9 **P2-1**-10

P2-3-9 **P2-3**-12 **P3-1**-8 **P3-1**-12

P3-2-5 **P3-2**-7 **P3-3**-10 **P3-3**-11

Figure 13. *(continued)* Typical failure modes of the tested samples: two specimens from each sample.

Preprints (www.preprints.org) | NOT PEER-REVIEWED | Posted: 28 June 2022 doi:10.20944/preprints202206.0382.v1

4. Effect of fibres

4.1. Qualitative evaluation

First the effect of fibres was noticed at the failure of the specimens. The failure mode was very brittle and close to explosive for the specimens with no fibres and no stirrups. Specimens with conventional stirrups had less brittle failure, but there was spalling of concrete cover observed. Specimens containing fibres showed very soft failure and had almost no concrete spalling.

In the case of FRC specimens the effect of thickness of concrete cover was noticed. Some of the specimens with the bar distance $c = 30$ mm had partial spalling of the concrete cover (see specimens P2-1-10 and P3-1-8 in Figure 13). It can be explained by the lack of fibres in the volume of the cover. Due to the relatively narrow space between the bars and surrounding moulds, the distribution of the fibres was disturbed.

4.2. Quantitative evaluation

The quantitative assessment of the fibre effect is done by evaluating correlation coefficients between fibre content V_f and the determined properties: maximum force, stiffness, and ductility. The relative and normalised values calculated by Equations (2), (4) and by the method given in Subsection 2.4.3 are used.

A profound negative correlation between nominal fibre content and relative maximum force was observed – the more fibres added, the smaller the maximum force. Correlation coefficients vary from -0.72 to -0.92 with p-value strongly below 0.05 value (see Figure 14). The average relative maximums force for specimens with fibres 30 kg/m^3 is 91%–93% and for specimens with 60 kg/m^3 is 84% of the maximum force of specimens with no fibres.

There is a very small or negligible correlation between the relative value of the overall stiffness and the amount of fibres observed. On average, the stiffness is smaller for specimens with fibres. The negative effect is more profound for samples with the smallest concrete cover (c = 30 mm) (see Figure 15).

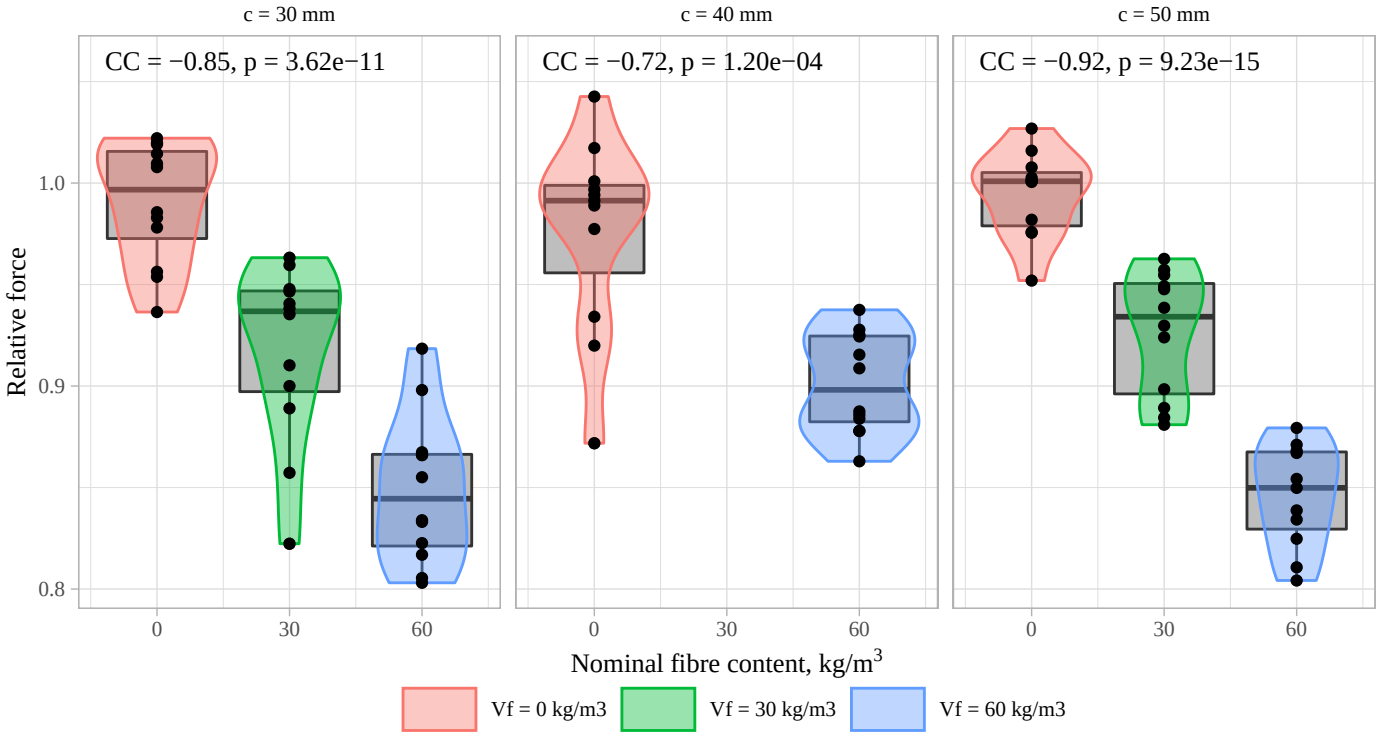

Figure 14. Correlation between maximum force (relative value) and fibre content.

Preprints (www.preprints.org) | NOT PEER-REVIEWED | Posted: 28 June 2022 doi:10.20944/preprints202206.0382.v1

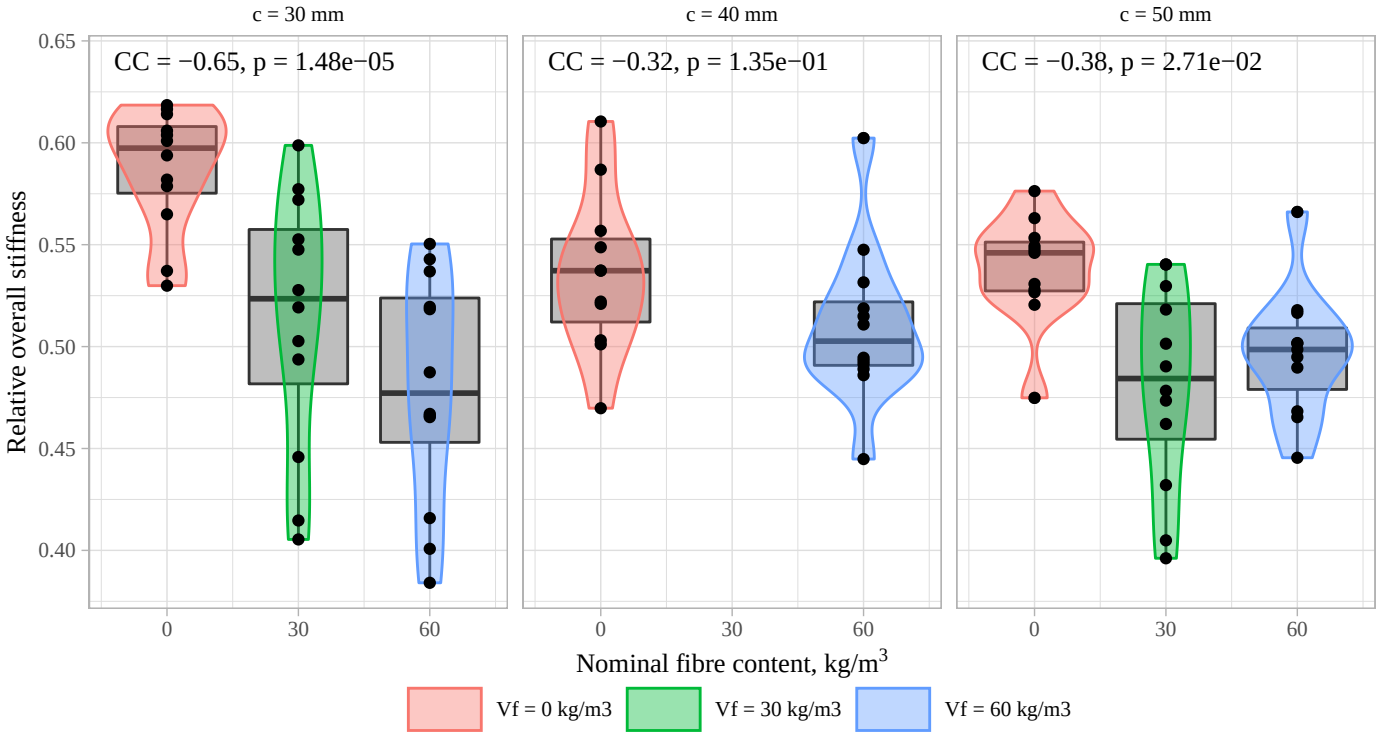

Figure 15. Correlation between stiffness (relative value) and fibre content.

As it was mentioned earlier, fibres increase ductility or the residual strength of the reinforced concrete elements. This property was estimated by comparing area under the normalised *force–displacement* curves. There is a positive correlation between the nominal amount of fibres and the area under normalised curves among the specimens in this study (see Figure 16). The increase is more profound for the sample with the highest fibre content (V_f = 60 kg/m^3). Unfortunately, the other two samples with the highest fibre dosage cannot be included in this evaluation, because of the different loading control approach used during the tests (see Subsection 2.4.3).

Specimens with conventional stirrups had increased ductility if concrete cover is rather small (Figure 17). The effect of the stirrups is equal to fibres with amount of 30 kg/m^3. However, the ductility was nearly the same as for the specimens with no fibres and no stirrups if the bar distance c = 50 mm. A reason for that could be the small distance between the bars, which was equal to 50 mm, thus the concrete volume between the bars or the core of the specimens is significantly smaller than the unreinforced volume outside the bars. On the other hand, fibres increased ductility also for specimens with the largest concrete cover.

The difference between the stirrups and fibres is that the ductility induced by stirrups depends on the volume enclosed by them, while its not the cases of SFRC. The ductility induced by fibres depends more on the distribution of fibres in the whole volume. Small concrete covers can disturb the distribution of fibres thus affecting other aspects as concrete spalling around the bars.

Analysis of variance (ANOVA) is used to estimate if fibres have had an influence on the scatter of the results. Variance between two parameters – coefficient of variation and presence of fibres – is evaluated. In case of overall stiffness *F value* is 11.67, which is greater than the critical value 5.317 (p-value: 0.0091 < 0.05). That means that the presence of fibres influences the scatter of the overall stiffness results. However, in case of maximum force and ductility (the area under *load-displacement* curve) no effect of the fibres to the coefficient of variation was found.

Preprints (www.preprints.org) | NOT PEER-REVIEWED | Posted: 28 June 2022 doi:10.20944/preprints202206.0382.v1

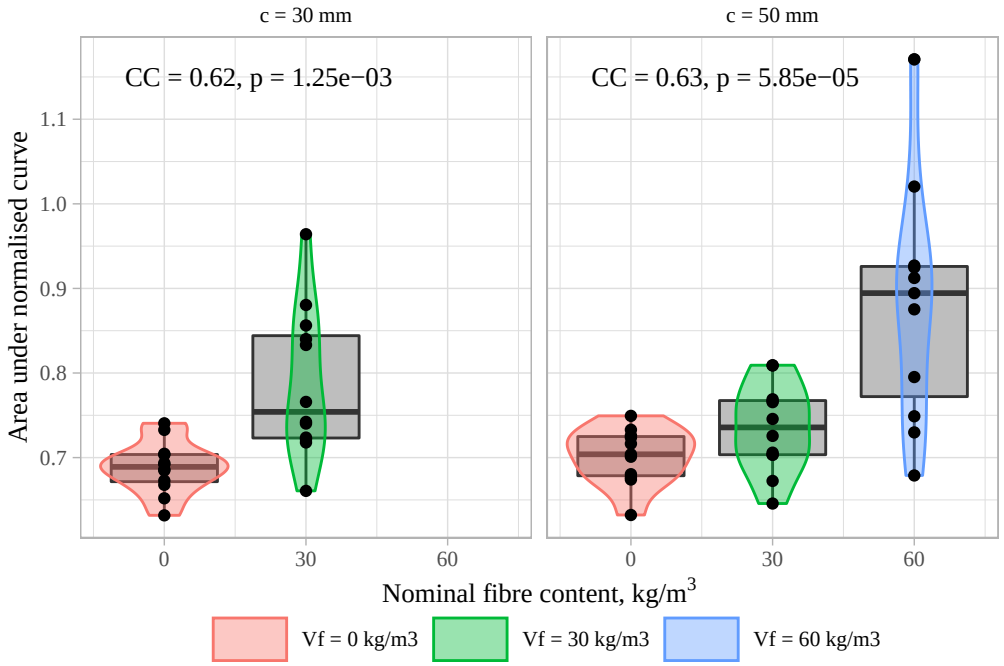

Figure 16. Correlation between area under normalised *force–displacement* curve and fibre content.

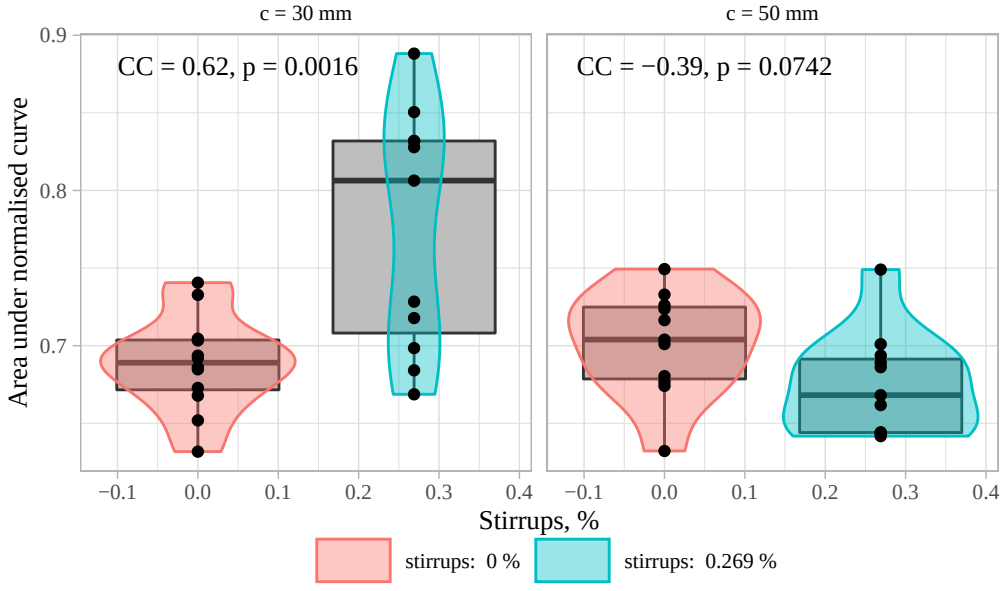

Figure 17. Correlation between area under normalised *force–displacement* curve and amount of stirrups.

4.3. Negative effect of fibres

The negative effect of fibres on the load bearing capacity is confusing as it contradicts the obtained cube compressive strength, which in our case is higher for SFRC specimens (see Figure 3 (a)). Findings by other authors also show that by adding steel fibres to concrete, compressive strength increases [15–17]. A possible explanation for the reduction is the disturbed compactness of concrete mix during casting process caused by the combination of re-bars and fibres. The specimens were made from self-compacting concrete with no vibration applied. Longitudinal re-bars create zones where the flow of concrete mix with 50 mm fibres is disrupted, leading to concrete sections with lower

 doi:10.20944/preprints202206.0382.v1

density. The discrepancy between the results of control cubes and the test specimens shows that the presence and arrangement of conventional reinforcement can affect the properties of SFRC considerably.

This complies with the detailing rules given in [7,8] providing for minimum spacing between re-bars, which in case of self-compacting concrete is suggested to be 1.5 to 2 times the fibre length. Current study suggests that additional rules for minimum concrete cover should also be included in the design of combined reinforced and fibre reinforced concrete structures.

Fantili et.al. [3] have given a theoretical example how a concrete column with steel fibres of 70 kg/m^3 would have the same ductility as column with minimum amount of conventional stirrups. Their calculation is based on an assumption that the effect of fibres in cylindrical specimens and columns with reinforcement bars is the same. It can be true for ductility of the cross-section but one must be cautious considering strength properties. Current study suggests that the arrangement of conventional reinforcement and thickness of concrete cover can have a negative influence to the effect of fibres.

5. Conclusions

In this experimental study the effect of steel fibres in compressed reinforced concrete elements was evaluated and compared to the effect of minimum required conventional horizontal ties. Ten different samples with 120 specimens in total were tested and the following conclusions can be drawn:

1. Specimens with plain concrete and longitudinal reinforcement only failed in nearly explosive manner due to the buckling of the re-bars. Specimens with minimum amount of stirrups failed in more ductile manner but spalling of concrete cover occurred. Failure of specimens with fibres and no stirrups was very soft and no spalling was observed.
2. If thickness of concrete cover is relatively small, fibres can be blocked from getting in the outer corners of the specimens. In such cases partial spalling of the concrete cover was observed due to the small amount of fibres in the region.
3. Specimens with fibre amount of 30 kg/m^3 showed similar ductility as the specimens with minimum amount of conventional stirrups. For specimens with large concrete covers and small core between longitudinal re-bars no effect of conventional stirrups on the ductility was observed, while the ductility caused by fibres remained profound.
4. There was a strong negative correlation (-0.72, -0.85, and -0.92) between nominal amount of fibres and the maximum compressive force carried by the test specimens. If compared to specimens with no fibres, the average maximum force was 92% and 84% for specimens with fibre content 30 and 60 kg/m^3, respectively.
5. Although no significant correlation was found, on average the specimens with fibres had smaller overall compressive stiffness if compared to those with no fibres. The presence of fibres increased also the scatter of the obtained stiffness values.
6. Combination of steel fibres and conventional re-bars as a reinforcement of concrete structures can lead to less qualitative compactness of the concrete if self-compacting concrete with no vibration is used. This can lead to reduction of stiffness and maximum load bearing capacity.

Funding: The research received funding from the European Regional Development Fund, Post-doctoral Research Support Program (project No.1.1.1.2/16/I/001) Research application "Efficiency of fibre reinforced cement composites in structural walls" (No.1.1.1.2./VIAA/3/19/487). Test specimens were produced and supplied by the project partner JSC "MB Betons".

Data Availability Statement: Publicly available datasets were analysed in this study. This data can be found here: https://www.llu.lv/lv/projektu_resursi/6274 under Work Package 1.

Conflicts of Interest: The funders had no role in the design of the study; in the collection, analyses, or interpretation of data; in the writing of the manuscript, or in the decision to publish the results.

References

1. Skadins U. Efficiency of fibre reinforced cement composites in structural walls (in Latvian). Available online: https://www.llu.lv/lv/projekti/apstiprinatie-projekti/2020/isskiedru-cementa-kompozitu-izmantosanas-efektivitate-nesoso (accessed on 27.06.2022).
2. Zhang Y., Harries K.A., Yuan W. Experimental and numerical investigation of the seismic performance of hollow rectangular bridge piers constructed with and without steel fiber reinforced concrete *Eng. Str.* **2013**, *48*, 255–265.
3. Fantilli A.P., Vallini P., Chiaia B. Ductility of fiber-reinforced self-consolidating concrete under multi-axial compression *Cem. Concr. Compos.* **2011**, *33*, 520–527.
4. Ganesan N., Ramana Murthy J.V. Strength and behaviour of confined steel fiber reinforced concrete columns *ACI Mater. J.* **1990**, *87*, 221–227.
5. Pereiro-Barceló J., Bonet J.L. Mixed model for the analytical determination of critical buckling load of passive reinforcement in compressed RC and FRC elements under monotonic loading *Eng. Str.* **2017**, *150*, 76–90.
6. Khandaker M. A. H., Sandeep P., Tanvir M. Axial Behavior of Columns Confined with Engineered Cementitious Composite *ACI Str. J.* **2022**, *119*, 67–76.
7. SFRC Consortium. *Design Guideline for Structural Applications of Steel Fibre Reinforced Concrete*; SFRC Consortium, 2014. Available online: http://www.steelfibreconcrete.com/34429 (accessed on 13.05.2022).
8. SIS Swedish Standard. *Fibre Concrete — Design of Fibre Concrete Structures*; Ref. No. SS812310:2014; Swedish Institute for Standards: Stockholm, Sweden, 2014.
9. CEN European Standard. *Testing hardened concrete - Part 3: Compressive strength of test specimens*; Ref. No. EN 12390-3:2019 E; CEN: Brussels, Belgium, 2019.
10. CEN European Standard. *Testing hardened concrete - Part 5: Flexural strength of test specimens*; Ref. No. EN 12390-5:2019 E; CEN: Brussels, Belgium, 2019.
11. CEN European Standard. *Test method for metallic fibre concrete - Measuring the flexural tensile strength (limit of proportionality (LOP), residual*; Ref. No. EN 14651:2005+A1:2007: E; CEN: Brussels, Belgium, 2007.
12. Fédération internationale du béton (fib). *Model Code 2010, final draft*; fib Bulletin Nos. 65/66; Lausanne, 2012.
13. CEN European Standard. *Eurocode 2: Design of concrete structures - Part 1-1: General rules and rules for buildings*; Ref. No. EN 1992-1-1:2004: E; CEN: Brussels, Belgium, 2004.
14. Campione C., Fossetti M., Maurizio P. Behavior of Fiber-Reinforced Concrete Columns under Axially and Eccentrically Compressive Loads. Technical paper. *ACI Str. J.* **2010**, *107*, 272–281.
15. Akbari C., Khalilpour S., Dehestani M. Analysis of material size and shape effects for steel fiber reinforcement self-consolidating concrete. *Eng. Fract. Mech.* **2019**, *206*, 46–63.
16. Abbass W., Khan M.I., Mourad S. Evaluation of mechanical properties of steel fiber reinforced concrete with different strengths of concrete. *Constr. Build. Mater.* **2018**, *168*, 556–569.
17. Zhang L., Zhao J., Fan C., Wang Z. Effect of Surface Shape and Content of Steel Fiber on Mechanical Properties of Concrete. *Adv. Civ. Eng.* **2020**, *2020*, 1–11.